Applied Surface Science 540 (2021) 148301

Contents lists available at ScienceDirect

Applied Surface Science

journal homepage: www.elsevier.com/locate/apsusc

The active site of ethanol formation from syngas over Cu_4 cluster modified MoS_2 catalyst: A theoretical investigation

Jiawang Chen [a,b], Zhanhui Wang [a], Juan Zhao [a], Lixia Ling [a,*], Riguang Zhang [b], Baojun Wang [b,*]

[a] College of Chemistry and Chemical Engineering, Taiyuan University of Technology, Taiyuan 030024, Shanxi, PR China
[b] Key Laboratory of Coal Science and Technology of Ministry of Education and Shanxi Province, Taiyuan University of Technology, Taiyuan 030024, Shanxi, PR China

ARTICLE INFO

Keywords:
Ethanol synthesis
MoS_2 catalyst
Reaction mechanism
Metal cluster
DFT

ABSTRACT

In order to clarify the active site of Cu_4 and MoS_2 on the conversion of syngas to ethanol over the Cu_4 cluster modified $MoS_2(001)$ [$Cu_4/MoS_2(001)$] surface, we have explored the reaction mechanism of ethanol formation by using density functional theory (DFT) method. It is concluded that CO is first hydrogenated to formyl (CHO) over the Cu_4/MoS_2 catalyst. The formed CHO is preferentially dissociated to form CH_2 by hydrogenation, which is the most favorable CH_x monomer. C-C bond is formed by CHO insertion into CH_2 leading to the C_2 oxygenate CH_2CHO, which results in the formation of C_2H_5OH by successive hydrogenation. The microstructure analysis shows that the Cu_4 cluster provides undissociated CO and CHO, while the interface between Cu_4 and MoS_2 promotes the dissociation of CH_2O to form CH_2 monomer and promotes the formation of ethanol C-C bond. This work can provide valuable information for the synergistic effect of Cu_4 cluster and MoS_2 to improve the selectivity of ethanol synthesis.

1. Introduction

Ethanol was an important material for the chemical and pharmaceutical industries, which had a wide range of applications as a potential fuel additive or hydrogen carrier for clean energy delivery fuel cells [1]. The catalysts used for syngas to form ethanol including four types: Cu-based catalysts [2–6], Rh-based catalysts [7–10], Mo-based catalysts [11–15], and modified Fischer-Tropsch synthesis catalysts [16–20]. Although Rh-based catalysts had a high selectivity for ethanol, they were not suitable for large-scale industrial applications due to the expensive cost [21]. Cu supported on ZnO and Al_2O_3 catalysts were used widely for the alcohol formation from syngas, however, these catalysts lose activity rapidly under the action of trace amounts of sulfides [22,23]. Therefore, the industry needed extra desulfurize process to reduce the sulfur to an extremely low level, which increased the product cost. The development of transition metal sulfide catalysts had become an effective way to solve this issue. Be distinguish from metal oxide catalysts, transition metal sulfide catalysts were not only resistant sulfur poison, but they had resistance to carbonization [24,25]. It was well known that the main product was hydrocarbon on the MoS_2 catalyst, it used to product alcohol after modification with alkali metal [26,27]. According to previous studies [28–30], the related reactions of syngas conversion on MoS_2(10–10) [28], MoS_2(1 1 0) [29], MoS_2(0 1 0) [29], MoS_2(1 0 0) [30] and MoS_2(0 0 1) [31] surfaces had been explored. The MoS_2 catalyst was conducive to the activation of CO, whereas, it was able to hydrogenate to form CH_4 instead of C_2 oxygenates via the C-O bond breaking to form CH_2 species. Therefore, the MoS_2 had the ability for activating CO to CH_x species, it was necessary to improve the activity by reduce the C_2 oxygenates formation energy barrier in order to promote the formation of C_2 oxygenates [32].

Surisetty et al. [33] have found that transition metal modified MoS_2 catalyst can catalyze the conversion of syngas to ethanol and alkanes. When the MoS_2 catalyst doped by heteroatoms, not only the in-plane inert sulfur was activated, but also adjusted the electronic structure and increased the molecular adsorption [34] During the hydrogenation of syngas on MoS_2 catalysts modified with K and Co, the two sulfur compounds Co_3S_4 and Co_9S_8 were formed by Co and MoS_2 combined. Co_9S_8 leaded to the decrease of catalyst activity, and its content increased with the increase of reaction time. On the other hand, Co and MoS_2 formed the Co-Mo-S structure, and the $Mo^{3.5+}$ component in the structure played a key role in alcohol formation [35–37] Researchers studied the hydrogen evolution reaction on Co-modified MoS_2 catalysts, the active site and effective active surface area were increased after adding Co [38].

* Corresponding authors.
E-mail addresses: linglixia@tyut.edu.cn (L. Ling), wangbaojun@tyut.edu.cn (B. Wang).

https://doi.org/10.1016/j.apsusc.2020.148301
Received 13 June 2020; Received in revised form 21 October 2020; Accepted 27 October 2020
Available online 4 November 2020
0169-4332/

Among the existing conventional catalysts for ethanol, Cu-based catalysts were received extensive attention due to their low price [39]. Previous research [40] showed the main product of syngas on Cu catalyst was methanol because the non-dissociative adsorption of CO, the C-O bond hard to break, so that the yields of CH_x was insufficient on Cu (1 1 1) [41] , (1 1 0) [42] and (1 0 0) [43] surfaces. However, CO inserted into CH_x to form C_2 oxygenates easily when CH_x species formed [40], which requires addition of additives [44] or support [45] to adjust the catalyst structure.

Recent experiments showed SiO_2-supported Cu catalyst had good selectivity of ethanol [3], CoCu [44–46], RhCu [4,47], and MnCu [48] catalysts increase the selectivity of C_2 oxygenates. Previous studies presented the activity of metal-supported catalysts were related closely to the structure [49,50]. There were many experimental [51–55] and theoretical studies [56–58] carried out on supported catalysts. For example, ZnO and ZrO_2 [52], TiC [53], MgO [54,55,57,58] and Al_2O_3 [59] catalysts studied extensively. The Al_2O_3-supported Cu_4 cluster catalyst was used for the CO_2 hydrogenate to methanol formation. Compared with $Cu/ZnO/Al_2O_3$ catalyst, the Cu_4 cluster was supported to reduce the reaction energy barrier and improve the turnover rate of methanol formation [51]. Rh_4 cluster supported by Al_2O_3 showed excellent catalytic performance for the conversion of syngas to C_2 oxygenates, the hydroxyl group provides by the Al_2O_3 carrier which improves the selectivity for C_2 oxygenates [59]. When Cu deposited on the χ-Fe_5C_2(5 1 0) surface, which had good selectivity for the formation of alcohols in syngas conversion at the interface between Cu and Fe_5C_2 [60]. As well as Co/CoO_x surface was favorable for the formation of alcohols, the CoO_x provided undissociated CO, the CH_x species was formed on the interface between Co and CoO_x [61]. Similar results were happened on the interface between Co and Co_2C, the undissociated CO preferred to be located in Co_2C, and Co promoted the CO to form CH_x species [17].

During the conversion of syngas to ethanol, CO hydrogenated to form formyl species, followed by hydrogenation and CO insertion. Previous studies had found that CO was inserted into CH_x to form CH_xCO on MoS_2 catalysts [7,62,63]. At the same time, researchers had investigated the reaction mechanisms for ethanol formation from syngas. It was reported that the OCCHO species was an important reaction intermediate in the formation of ethanol on Cu(2 1 1) surface [2]. In addition, several researchers had experimental investigated that OCCOH formed by CO coupling and hydrogenation, which had the potential to form C_2 oxygenates [64,65]. Based on the above analysis, a large number of studies proved that CH_x is an important reaction intermediates in the process of ethanol synthesis, which is coupled with CO or CHO to form C_2 oxygenates. Despite the recent research has reviewed in the progress of syngas to form ethanol directly, there is no generally accepted theory about the mechanism.

In this work, we studied the mechanism of ethanol synthesis on Cu_4/MoS_2 catalyst compared with pure Cu and MoS_2 catalysts. Meanwhile, the role of Cu_4 cluster and MoS_2 in the reaction process were discussed. The reaction mechanism of syngas conversion to ethanol was systematically studied on Cu_4/MoS_2 catalyst. We listed the research contents: illustrated the initial activation of CO, described the generation of CH*x* (*x* = 1–3) species, discussed the new path of C_2 oxygenates formation and surveys of microstructure analysis. Furthermore, the synergistic effect between Cu and MoS_2 was determined by comparison with Cu and MoS_2 catalysts.

2. Calculation details

2.1. Calculation methods

The Vienna Ab Initio Simulation Package (VASP) [66–68] was employed for all calculations. The generalized gradient approximation (GGA) with Perdew-Burke-Ernzerhof (PBE) was used for the exchange–correlation functional [69]. The Brillouin zone was sampled using a 2 × 2 × 1 Monkhorst-Pack *k*-point grid with the Methfessel-Paxton smearing of 0.2 eV [31,70]. The plane-wave cut off energy was set with 400 eV to describe the electronic wave functions. The geometry optimization was allowed to converge when the energy difference between two consecutive steps was less than 1×10^{-5} eV, and the forces on each atom was lower than 0.03 eV·Å^{-1}.

Transition states were located by combining the Climbing Image Nudged Elastic Band method (CI-NEB) and Dimer method [71–74]. In this study, the forces for all the atoms of the optimized transition state structure using the dimer method were less than 0.05 eV·Å^{-1}. The transition states were further confirmed by a vibrational frequency calculation, in which only one imaginary frequency was obtained at the saddle points.

The binding energy value E_b is defined as,

$$E_b = E_{Cu_4-MoS_2} - E_{Cu_4} - E_{MoS_2} \tag{1}$$

where $E(Cu_4/MoS_2)$, $E(Cu_4)$ and $E(MoS_2)$ are the total energies for the Cu_4/MoS_2(0 0 1), the Cu_4 cluster, and the MoS_2 with vacancy, respectively.

For the reaction molecules adsorbed on the catalyst, the adsorption energy (E_{ads}) is determined by,

$$E_{ads} = E_{A/slab} - E_A - E_{slab} \tag{2}$$

where *E*(A/slab), *E*(A) and *E*(slab) are total energies of the molecules/catalyst, the reaction molecule, and the isolate catalyst.

The reaction energy (ΔE) and activation energy (E_a) are defined as

$$E_a = E_{TS} - E_{IS} \tag{3}$$

$$\Delta E = E_{FS} - E_{IS} \tag{4}$$

where *E*(IS), *E*(TS), and *E*(FS) are the total energies of the reactant, transition state and product, respectively.

The activation barrier with the zero-point correction is calculated on the basis of the equations (5) and (6),

$$\Delta E_a = (E_{TS} - E_{IS}) + \Delta ZPE_{barrier} \tag{5}$$

$$\Delta ZPE_{barrier} = \left(\sum_{i=1}^{Vibration} \frac{hf_i}{2}\right)_{TS} - \left(\sum_{i=1}^{Vibration} \frac{hf_i}{2}\right)_{IS} \tag{6}$$

where $\Delta ZPE_{\text{barrier}}$ refers to the zero-point energy correction for the reaction barrier, h and f_i refer to Planck's constant and vibration frequency.

In order to exploring the temperature effect during syngas conversion, the rate constant was investigated by Transition State Theory (TST), the equation can be expressed as following,

$$k = v_i exp\left(\frac{-\Delta E_a}{RT}\right) \tag{7}$$

$$v_i = \frac{k_B T}{h} \frac{\prod_{i=1}^{3N}\left[1 - exp\left(-\frac{hf_i^{IS}}{k_B T}\right)\right]}{\prod_{i=1}^{3N-1}\left[1 - exp\left(-\frac{hf_i^{TS}}{k_B T}\right)\right]} \tag{8}$$

where R is the gas constant. k_B is the Boltzmann's constant and the T refers to the reaction temperature under experimental conditions.

2.2. Surface model

For the MoS_2 catalyst, the trigonal antiprismatic phase (1 T-MoS_2), hexagonal prismatic phase (2H-MoS_2) and rhombohedral phase (3R-MoS_2) has exist. Reshmi et al. [75] experimentally found that 2H-MoS_2 had the best stability. Moreover, the research on 2H-MoS_2 phase mainly focused on MoS_2(0 1 0), (0 0 1) and (1 1 0) surfaces, the (0 0 1) surface

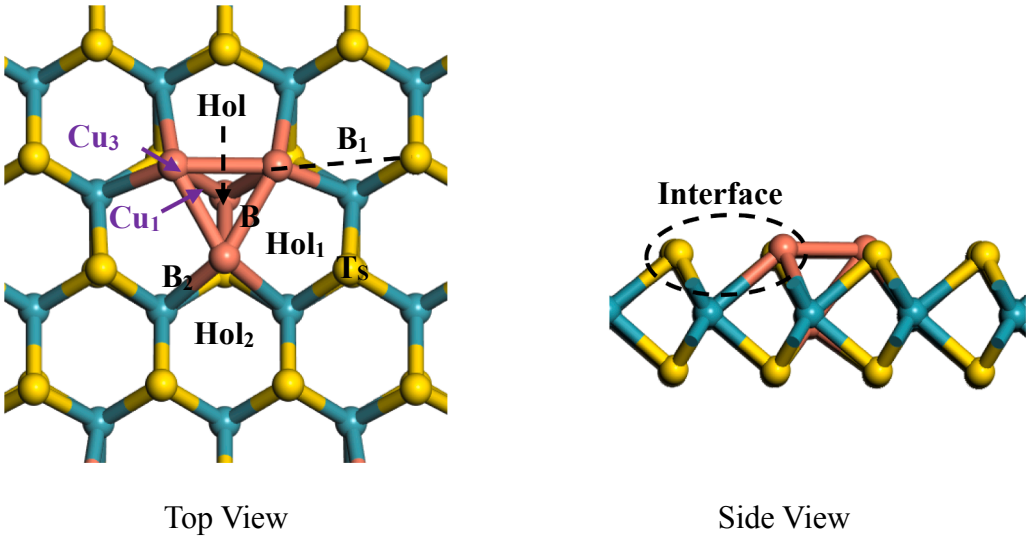

Fig. 1. The top and side views of $Cu_4/MoS_2(001)$ surface; the orange, yellow and cyan spheres represent Cu, S and Mo atom, respectively. One Cu atom taking the place of the Mo atom is named as Cu_1, and the other three Cu atoms substituting three S atoms on the surface of monolayer MoS_2 are called Cu_3. H, B and T represent the Hcp, Bridge and Top site, respectively. T_S, B_1, B_2, Hol_1 and Hol_2 represent the Top, Bridge and Hol site of the interface, respectively. (For interpretation of the references to colour in this figure legend, the reader is referred to the web version of this article.)

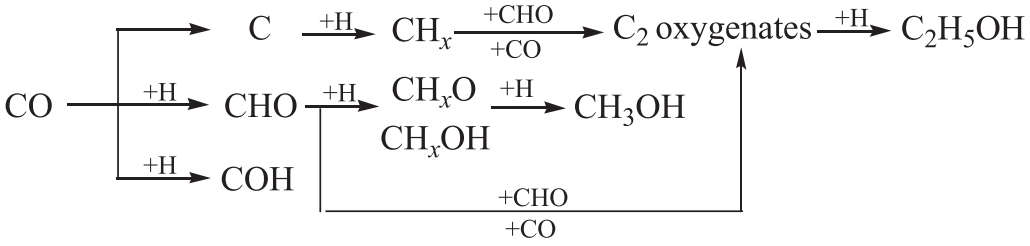

Scheme 1. The possible paths for syngas conversion on the $Cu_4/MoS_2(001)$ surface.

was the most stable, having a relative abundance (total facet area fraction) of 99% [29]. The studies by Wang and Zhang focused on the several reactions on $MoS_2(001)$ including the hydrodesulfurization of gasoline [76]. and HER reaction [77]. Among these studies, the (001) surface was given special attention as it was the lowest energy surface of MoS_2. Further, Zhang et al. [31] theoretically investigated syngas conversion to methane over the $MoS_2(001)$ surface, suggested that the S-terminated $MoS_2(001)$ may be easily dissociated CH_2OH to form CH_2.

As a common metal, Cu has a low price and a high activity for syngas conversion reaction. After modified by Cu_4, the original structure of MoS_2 was changed to improve the catalytic activity. One Mo atom and three S atoms in the single layer MoS_2 can be replaced by Cu_4 clusters to form a stable Cu_4 modified MoS_2 catalyst. Therefore, the model was built to size of $p(3 \times 3)$ and a vacuum layer of 15 Å for $MoS_2(001)$ surface with one bottom monolayer relaxed. Cu_4 cluster was substituted for the three S on the surface and Mo connected to the subsurface layer to obtain stable Cu_4 embedded in an inverted triangular pyramid, the model on the $MoS_2(001)$ surface was denoted as: $Cu_4/MoS_2(001)$ structure, this stable model had been used for the study of CO oxidation.

The structure of Cu_4/MoS_2 is shown in Fig. 1. There are nine sites on the $Cu_4/MoS_2(001)$ surface, One Cu atom taking the place of the Mo atom is named as Cu_1, and the other three Cu atoms substituting three S atoms on the surface of monolayer MoS_2 are called Cu_3. T, B and Hol represent the Top, Bridge and Hollow sites on Cu_4 cluster; T_S present the top site of S atom; B_1, B_2, Hol_1 and Hol_2 represent the Bridge and Hollow sites at the interface, respectively. B_1 represents Bridge site composed of one surface Cu atom and one surface S atom; B_2 represents another Bridge site composed of one surface Cu atom and one subsurface Mo atom; Hol_1 presents the 3-fold hollow site which formed by two S atoms and one Mo atom; Hol_2 means a different 3-fold hollow site consist one S atom and two Mo atoms. In order to gain a deeper understanding of the single-layer MoS_2 modified with Cu_4 cluster, the binding energy (E_b) $E_fE_f$is calculated, as shown in Eq. (1). The energy is −7.89 eV, which indicated that there is a strong interaction between Cu_4 clusters and single-layer MoS_2.

3. Results and discussion

In general, the process of ethanol formation involves two key steps, namely, CO activation and carbon chain growth, as shown in Scheme 1. We also consider other possible reaction paths on the $Cu_4/MoS_2(001)$ surface via syngas conversion, which helps us to understand the catalytic performance of Cu_4/MoS_2 catalyst.

3.1. CO hydrogenation and dissociation

Previous research [78] shows that the unique triangular active site is the significant site where the CO adsorbed, and it is identified as a crucial role for CO activation [81]. We investigate all possible reaction sites of CO adsorption and we find that CO is stably adsorbs at the Top site of Cu_3 triangular active site, Chen's results [79] show that CO can be stably adsorbed on the top sites of Cu_4 clusters on MoS_2 catalyst doped with Cu_4 clusters, and the adsorption energy is 1.095 eV, which is similar to our results.

In Fig. 2, the initial activation of CO involves direct dissociation, formation of CHO or COH species under H-assisted. Starting from the adsorbed CO and H, the CO + H adsorb at T_1 and H_1 site, respectively, the distance between C and H atoms reduce to 1.119 Å in CHO from 2.737 Å in initial state via 1.274 Å in TS 1. This path needs to overcome the reaction barrier of 111.0 kJ·mol^{-1}, and is lower than that of the reaction pathways of CO + H → COH (268.0 kJ·mol^{-1}) and CO → C + O (496.1 kJ·mol^{-1}). We obtain the information that CO + H → CHO is the main pathway for CO activation, which agrees well with the investigation on Cu(1 1 1), MoS_2(0 1 0), and MoS_2(0 0 1) surfaces [41,29,70]. The

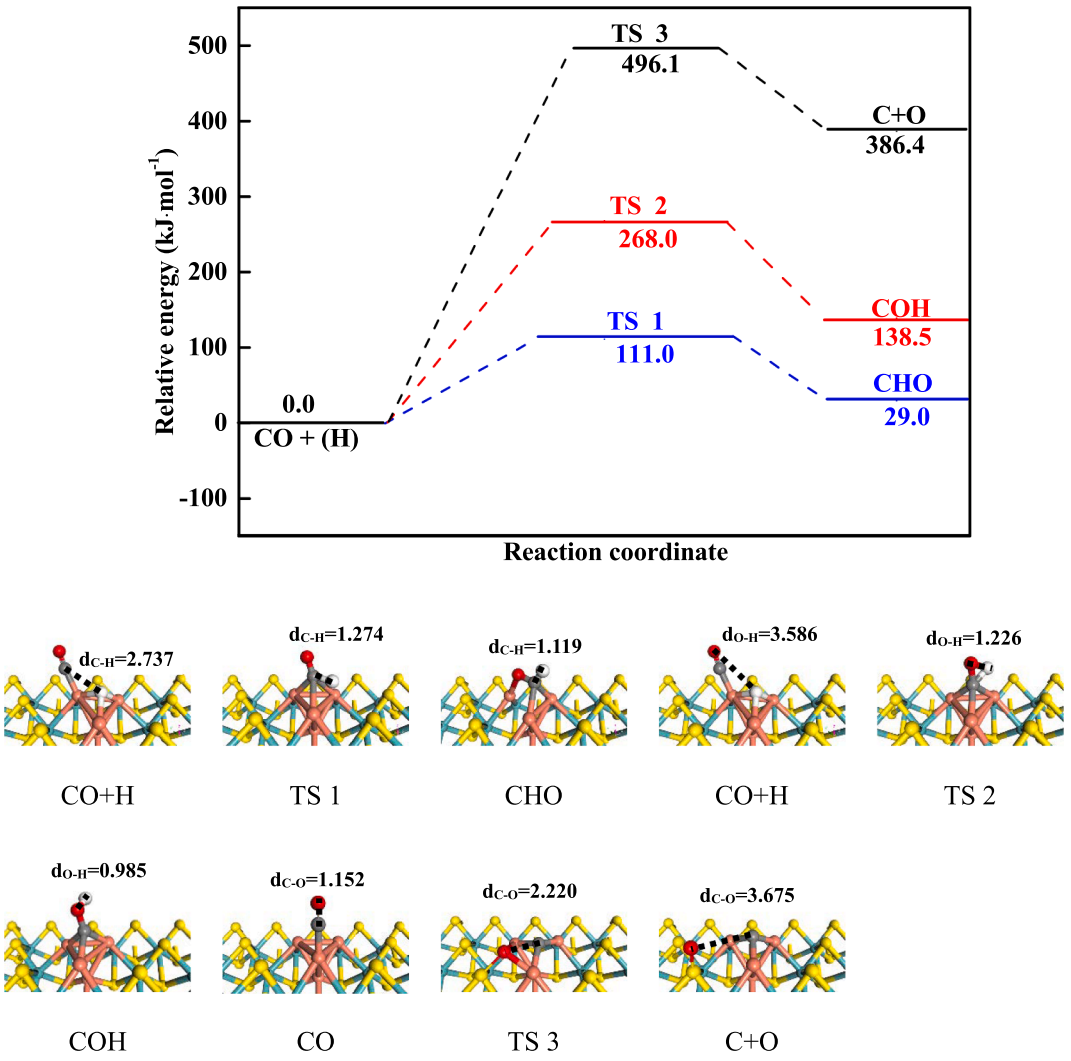

Fig. 2. The potential energy profile for CO activation with the structures of the initial states (IS), transition states (TS), and final states (FS). The unit of bond length in all structure diagrams is Å.

energy barrier of forming CHO on $Cu_4/MoS_2(001)$ is 110.0 kJ·mol^{-1} which is similar to that on the Cu(111) surface with 105.8 kJ·mol^{-1} [41], it is greatly lower than that on the MoS_2 (010) and (100) surfaces with 166.9 and 165.0 kJ·mol^{-1}, respectively [29,30].

3.2. CH_x formation and related reactions

Starting from CHO, the formation of CH_x (x = 1–3) includes two pathways: CH_xO direct or H-assisted dissociation, and CH_xOH (x = 1–2) dissociation.

3.2.1. CH_x(x = 1–3) and methanol formation

This section contains a discussion about the formation of CH, CH_2, CH_3 and methanol, the detail potential energy profile is presented in Figs. 3–6. The following is the pathways for the formation of CH_x (x = 1–3) species and methanol.

The process of CH formation includes two paths, one is CHO hydrogenates to form CHOH with the reaction barrier of 51.4 kJ·mol^{-1}, and then CHOH dissociates to form CH and OH, which needs overcome a reaction barrier of 137.3 kJ·mol^{-1} with a reaction heat of 43.3 kJ·mol^{-1}. The other is the direct dissociation of CHO to CH and O, a very great energy barrier is needed to be overcome with 286.7 kJ·mol^{-1}.

As depicted to form CH_2 species, the progress contains three types, namely, CHO hydrogenates to form CH_2O and then dissociate under H-assisted to form CH_2 and OH. In this path, CH_2O is at Hol site and H atom adsorbs in T_S site, the distance between H and O atom is 3.942 Å in original state. Then, O atom in CH_2O moves toward H atom, the distance between O and H atoms decrease to 1.006 Å in final state via 2.137 Å in TS 9, with a higher barrier of 77.4 kJ·mol^{-1}, accompanied by reaction heat of 34.1 kJ·mol^{-1}. The activation barrier of CH_2 formation is remarkably lower than a previously reported corresponding barrier via CH_2OH dissociation to form CH_2 and OH [80] and the direct dissociation of CH_2O.

For CH_3 formation, CH_3O is formed by continuous hydrogenation of CHO and it dissociates to form CH_3 and OH under H-assisted dissociation. The path of CH_3O dissociation needs to conquer the higher reaction barrier of 194.6 kJ·mol^{-1}. For the formation of methanol, the preferred route is CHO continuously hydrogenated to form methanol, with the activation barrier and reaction energy of 137.1 and −144.0 kJ·mol^{-1}, respectively. The reaction barrier of the methanol formation on Cu_4/MoS_2 is higher than that of Co-modified MoS_2 catalysts, simultaneously, both reactions release plentiful heat [81].

It can be seen that CH_2 is the most important CH_x(x = 1–3) monomer, and the key step of CH_2 formation is $CH_2O + H \rightarrow CH_2 + OH$, with an energy barrier of 77.4 kJ·mol^{-1}. The key step of methanol formation is $CH_2O + H \rightarrow CH_2OH$, with an energy barrier of 137.1 kJ·mol^{-1}. The formation of CH_2 monomer was more favorable than methanol generation.

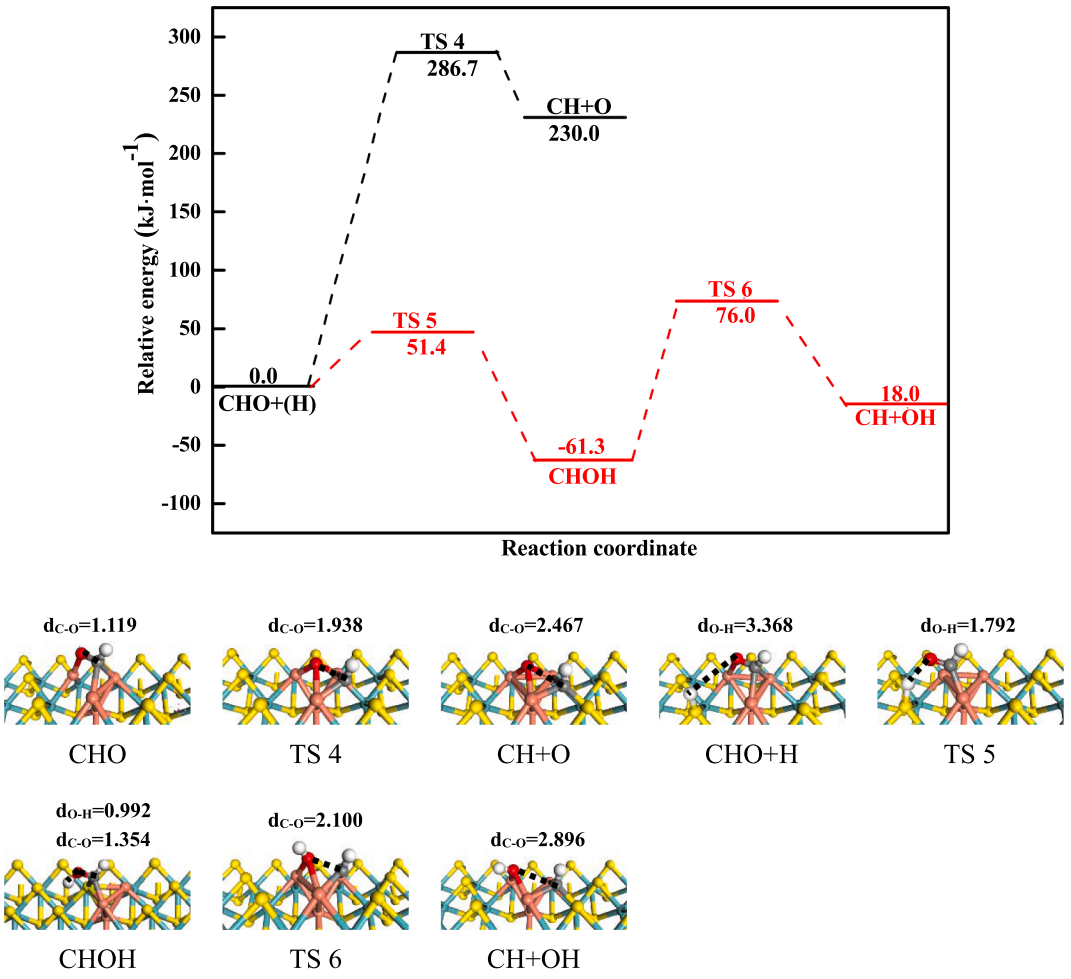

Fig. 3. The potential energy profile for CH formation with the structures of the initial states (IS), transition states (TS), and final states (FS) on $Cu_4/MoS_2(001)$ surface.

3.2.2. CH_2 related reactions

In this section, we focus on the related reactions of CH_x. The above research shows that CH_2 is the most favorable CH_x monomer on $Cu_4/MoS_2(001)$ surface. The related reactions of CH_2 includes three elementary reactions are shown in Fig. 7. CH_2 hydrogenates to CH_3 has an activation energy of 104.1 kJ·mol^{-1}. The C_2 oxygenates formation includes two paths, namely CHO or CO insertion into CH_2. For the prior, the co-adsorption configuration of CHO and CH_2 coupling through C-C via TS 18 to form a stable intermediate CH_2CHO at Hol site on the $Cu_4/MoS_2(001)$ facet, the distance between two C atoms reduce to 1.380 Å at final state from 3.627 Å in original state, which needs to overcome a barrier of 66.0 kJ·mol^{-1}, and the reaction heat is −278.9 kJ·mol^{-1}. For the later, starting from co-adsorbed CH_2 and CO, CH_2 at Hol_1 and CO adsorbs in T site, the distance between two C atoms is 2.889 Å in original state. Then, CO moves toward CH_2, and CO stays at Hol site, the length of C-C band decreases to 1.384 Å in CH_2CO via 2.045 Å in TS 19, whose activation barrier is 49.2 kJ·mol^{-1}, with the reaction heat is −80.5 kJ·mol^{-1}. Above results show that among all reactions related to CH_2, the formation of CH_3 is more difficult than that of CH_2CHO and CH_2CO, and the reactions of CH_2CHO and CH_2CO formation are competitive reaction, the reaction barriers of CH_2CHO and CH_2CO formation (66.0 and 49.2 kJ·mol^{-1}) are lower than that of CH_2CO formation on $Mo_{20}S_{43}$ cluster (212.3 kJ·mol^{-1}) [32], and lower than that of CH_3CO formation on MoRh(1 1 1) surface (101.3 kJ·mol^{-1}) [82].

3.3. C_2 oxygenates formation via CO/CHO-CHO coupling path

Based on previous research [64,65,83], the important reaction for C_2 oxygenates formation includes the hydrogenation of CO to CHO, then CHO coupling with CO or CHO on Cu-based catalyst. As presented in Fig. 8, the CHO adsorbs at Hol site, which overcomes the barrier of 32.8 kJ·mol^{-1} to attack the another to form OHCCHO, the distance between the two C atoms decreased to 1.435 Å in final state from 2.507 Å in the initial state. This step is obviously easier on $Cu_4/MoS_2(001)$ than that on the Cu/γ-AlOOH(001) surface, the latter needs to overcome the reaction barrier of 103.2 kJ·mol^{-1} [83]. Alternatively, C_2 oxygenates formation via the coupling reaction between CHO and CO is also considered. The formation of OCCHO is exothermic by 5.1 kJ·mol^{-1}, with the activation barrier of 93.9 kJ·mol^{-1}. Then, OCCHO hydrogenates to form OHCCHO, this step needs to conquer the activation barrier of 20.1 kJ·mol^{-1}. Starting with OHCCHO, the generated CHCHO resides in the Hol and O atom remains at T_S site, the distance between C and O atoms increases to 3.070 Å, whose activation barrier is 225.6 kJ·mol^{-1}, accompanied with the endothermic by 84.9 kJ·mol^{-1}.

Therefore, on the $Cu_4/MoS_2(001)$ surface, the C_2 oxygenates formation mainly depends on the CO or CHO inserts into CH_2 to form CH_2CO or CH_2CHO due to the lower activation barrier, rather than OHCCHO dissociates to form CHCHO.

3.4. Hydrogenation of C_2 oxygenates to form ethanol

In this part, we present the ethanol generates from C_2 oxygenates in

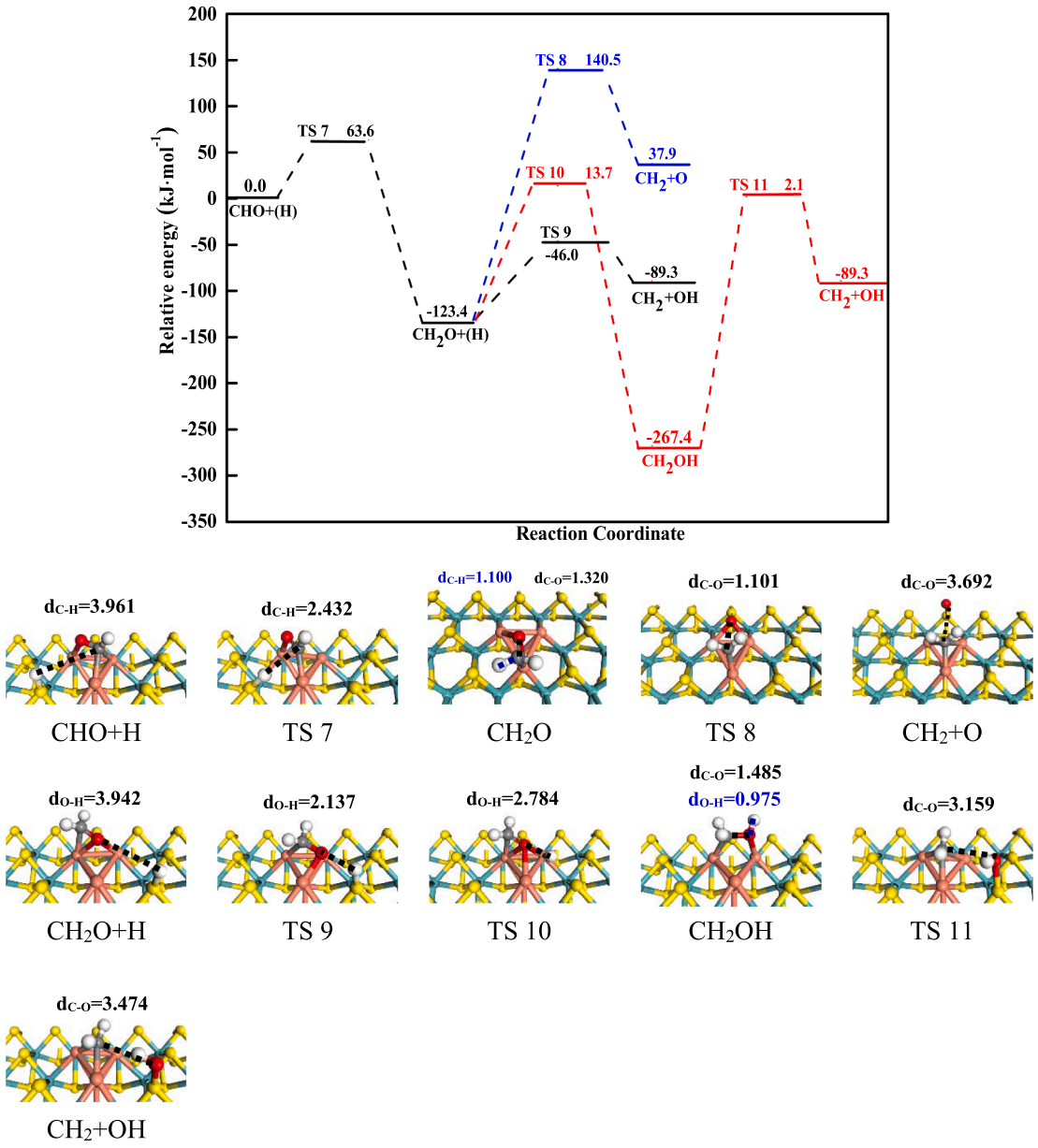

Fig. 4. The potential energy profile for CH_2 formation with the structures of the initial states (IS), transition states (TS), and final states (FS) on $Cu_4/MoS_2(001)$ surface.

the Fig. 9, it shows the reaction path for the ethanol formation. Starting from CH_2 species, the activation energy barrier of CH_2 combined with CHO to form CH_2CHO reaction is 66.0 kJ·mol^{-1}. Meanwhile, CH_2 inserts into CO to form CH_2CO is also considered here, the formation of CH_2CO is exothermic by 80.5 kJ·mol^{-1}, with an activation barrier of 49.2 kJ·mol^{-1}. Furthermore, our calculation shows that CH_2CO prefers to be hydrogenated to CH_2CHO, this route has the reaction barrier of 154.9 kJ·mol^{-1}, which needs to be exothermic by 212.5 kJ·mol^{-1}. Besides, CH_2CO hydrogenates to form CH_3CO, which needs to overcome a barrier of 155.8 kJ·mol^{-1}, the reaction heat is −175.1 kJ·mol^{-1}. The rate-limiting step barrier of CH_2CO hydrogenates to form CH_3CO or CH_2CHO are 155.8 or 154.9 kJ·mol^{-1}, respectively. The rate-limiting reaction barrier of CH_2CO relevant reactions is higher than that of the CH_2 directly insertion CHO, we can conclude that the CH_2CHO is the most favorable C_2 oxygenates. Above results show that the CHO reaction with CH_x is a more favorable route for C_2 oxygenates formation rather than the CO insert into CH_x, which is consistent with that over the Rh (111) [7] and (211) [84] surfaces. In contrast, our results on Cu_4/MoS_2 catalyst show that CH_3CHO formation via TS 26 with a very small activation barrier of 57.9 kJ·mol^{-1}, which is lower than that of on Cu (111) [41] surface (72.6 kJ·mol^{-1}). Subsequently, CH_3CHO hydrogenation to CH_3CH_2O via TS 27, this reaction energy barrier is 58.2 kJ·mol^{-1} with reaction energy of −273.7 kJ·mol^{-1}. Finally, the CH_3CH_2O hydrogenation to form ethanol needs to overcome the activation energy barrier of 82.3 kJ·mol^{-1}, accompanied a reaction energy by −42.9 kJ·mol^{-1}.

3.5. Selectivity of syngas to ethanol on Cu_4/MoS_2 catalyst

3.5.1. Selectivity of ethanol on Cu_4/MoS_2 catalyst

On the Cu_4/MoS_2, CO is activated by hydrogenation to form CHO, which is consistent with that on MoS_2(100) [30] and (001) [31] surfaces. It has a similar reaction barrier (109.0 and 105.8 kJ·mol^{-1}) with CO activation on MoS_2(100) [30] and Cu(111) [41] surfaces, but lower than that on MoS_2(010) [29] surface.

After the formation of the common intermediate CHO, the process of

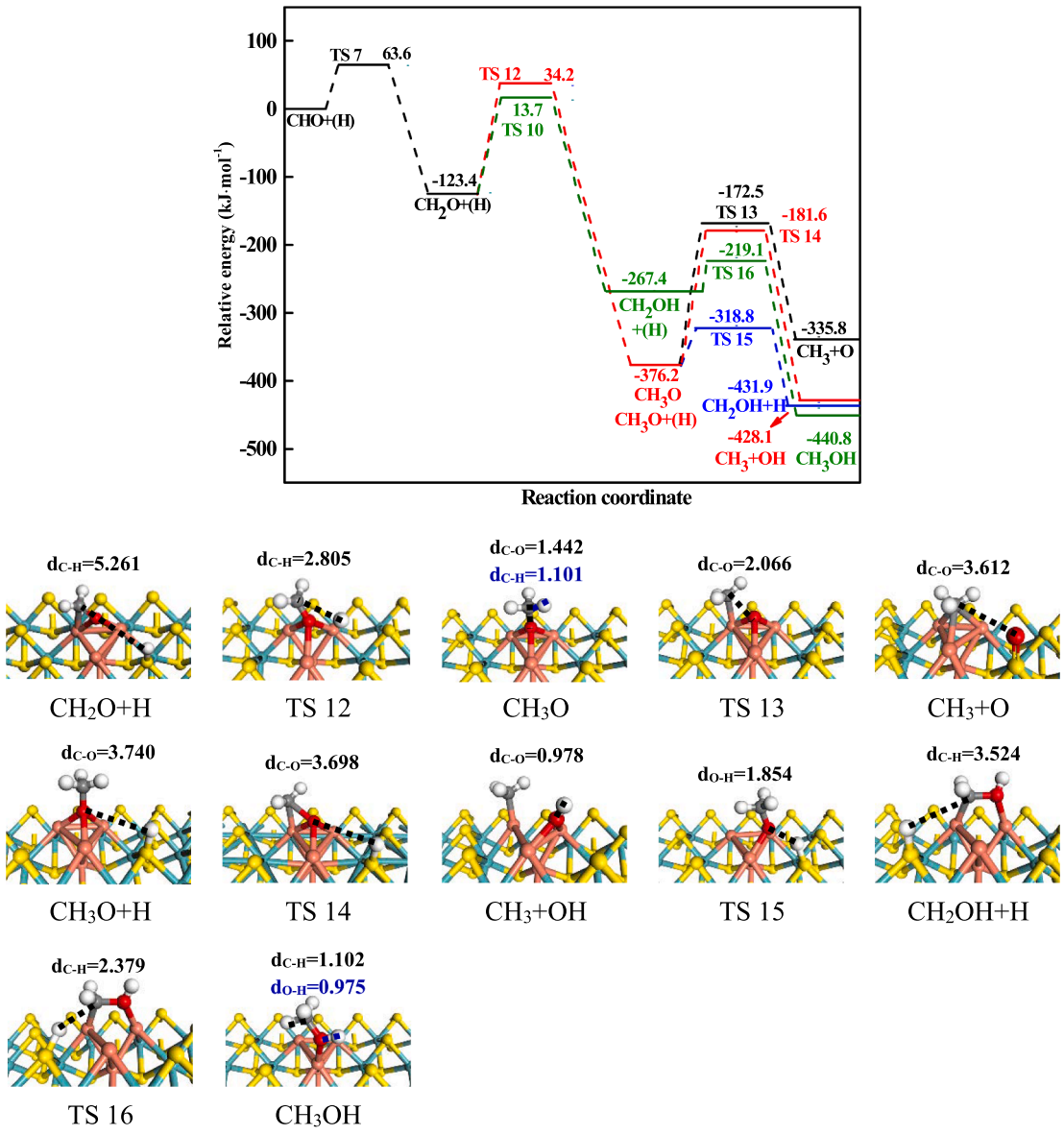

Fig. 5. The potential energy profile for CH_3 and CH_3OH formation with the structures on $Cu_4/MoS_2(001)$ surface.

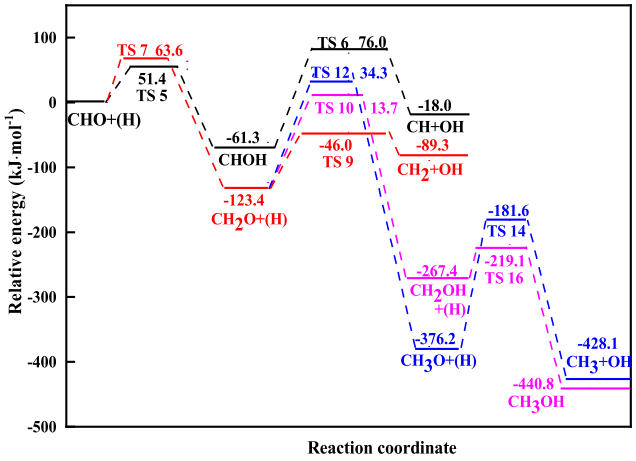

Fig. 6. The potential energy profile for CH_x and methanol formation with the structures of the initial states (IS), transition states (TS), and final states (FS).

forming the possible products ethanol and methanol are studied. The optimal path to form ethanol is $CHO + H \rightarrow CH_2O$; $CH_2O + H \rightarrow CH_2 + OH$; $CH_2 + CHO \rightarrow CH_2CHO$; $CH_2CHO + H \rightarrow CH_3CHO$; $CH_3CHO + H \rightarrow CH_3CH_2O$; $CH_3CH_2O + H \rightarrow C_2H_5OH$. In the process, the maximum activation energy required for the hydrogenation of CH_3CH_2O to form ethanol is 82.3 kJ·mol^{-1}.

Different from Cu-based catalysts, the optimal path for ethanol formation on the Cu(111) [41] surface by our previous study is CHO hydrogenation to form CH_2OH, subsequently, CH_2 prefers to be formed by CH_2OH dissociation. Since CH_2 inserted into CO to form CH_2CO, which was the main C_2 oxygenates on Cu(111) [41] surface, but CH_2CHO is the main C_2 oxygenates on $Cu_4/MoS_2(001)$. However, starting from CHO, the maximum energy barrier for the formation of ethanol is the same as that for the hydrogenation of CH_3CH_2O to form ethanol. On the Cu_4-MoS (001) and Cu(111) [41] surfaces, the reaction energy barriers in this step is 82.3 and 124.3 kJ·mol^{-1}, respectively.

For methanol generation, the most favorable reaction path is $CHO + H \rightarrow CH_2O$; $CH_2O + H \rightarrow CH_2OH$; $CH_2OH + H \rightarrow CH_3OH$. In this path, the $CH_2O + H \rightarrow CH_2OH$ requires the maximum activation energy which is 137.1 kJ·mol^{-1}. By comparing the energy barrier generated by ethanol and methanol (Fig. 10), the activation energy required for the

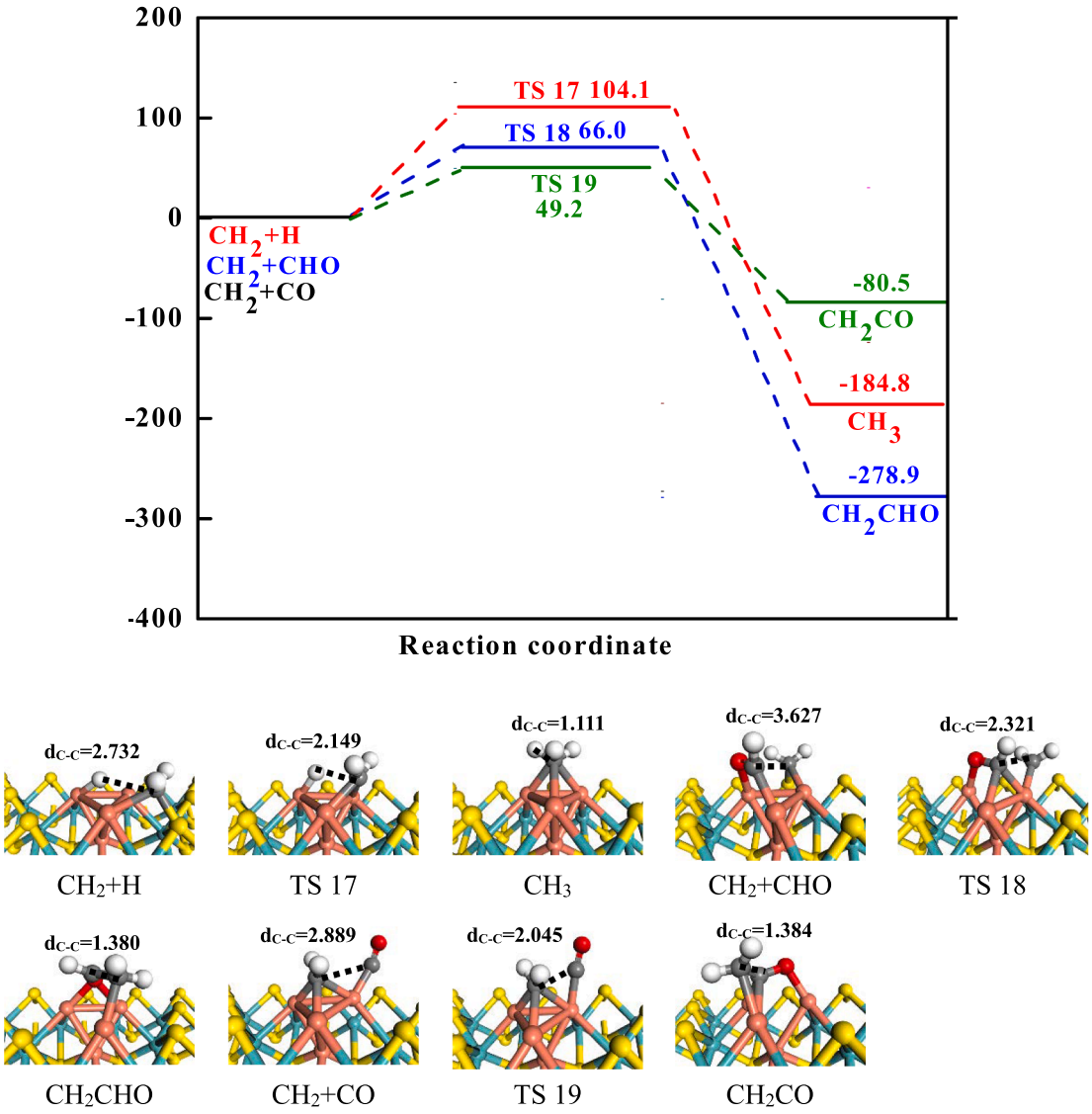

Fig. 7. The potential energy profile for CH_2 and CH_3 relate reactions with the structures of the initial states (IS), transition states (TS), and final states (FS).

formation of ethanol is the minimum. Therefore, ethanol is the main product on the $Cu_4/MoS_2(001)$ surface.

3.5.2. *Rate constants analyzation*

In order to further explore the selectivity of syngas conversion products on $Cu_4/MoS_2(001)$ catalyst, MoS_2 catalyst showed good catalytic activity in the temperature's range of 673–923 K, and the reaction rate constants of key elementary reactions at different temperatures were calculated (Table 1).

As depicted in Table 1, the rate constants (s^{-1}) in the range of 673–923 K are listed. As the initial intermediate involved in syngas conversion into the possible liquid products C_2H_5OH and CH_3OH, the rate constants of CHO species formation are in the range from 3.64×10^{-1} to 7.82×10^{1} along with the temperature range of 673–923 K. In addition, the relationship between stabilization of the product and reaction turnover has been analyzed to illustrate the selectivity of products. We investigate the relationship between the activation energies and adsorption energies (Table 2) of different products produced by the same intermediate through different elementary reactions. Through optimal path analysis, it can be found that with the same intermediate CH_2O as the demarcation point, methanol and ethanol are generated through different elementary reactions. The adsorption energy of CH_2OH produced by the hydrogenation of CH_2O is -205.6 kJ·mol^{-1}, which is a key intermediate for the formation of CH_3OH, while the adsorption energy of CH_2 formed by the dissociation of CH_2O is -345.6 kJ·mol^{-1}, which shows that the adsorption of CH_2 on the catalyst is more greater than CH_2OH. Moreover, the activation energy required for the formation of CH_2 is 77.4 kJ·mol^{-1}, and the corresponding rate constant at 673 K is 1.69×10^{3}. While the energy barrier for the hydrogenation of CH_2O to form CH_2OH is 137.1 kJ·mol^{-1} with a rate constant of 2.23×10^{0} at 673 K. In the subsequent reaction, from the common intermediate CH_2, CH_2CHO is formed via CHO inserting into CH_2, which will lead to the formation of ethanol. The adsorption energy of CH_2CHO is -262.8 kJ·mol^{-1} with an activation energy of 66.0 kJ·mol^{-1} for this insertion reaction forming CH_2CHO, and the corresponding rate constant at 673 K is 7.52×10^{2}. And the adsorption energy of CH_3 formed by the hydrogenation of CH_2 is -218.9 kJ·mol^{-1}. The activation energy of this step is 104.1 kJ·mol^{-1}, and the rate constant is 3.34×10^{0} at 673 K. It can be seen that CH_2CHO formation is more favorable than the formation of CH_2OH and CH_3 according to activation energies and rate constants, which will lead to the higher selectivity to C_2H_5OH than CH_3OH and the related products of CH_3 for syngas conversion. Thus, it can be seen that the stronger stabilization of the reaction product which has greater the absolute value of adsorption energy, the smaller the activation energy is required to form the product, and the higher reaction turnover of the elementary reaction. This is consistent

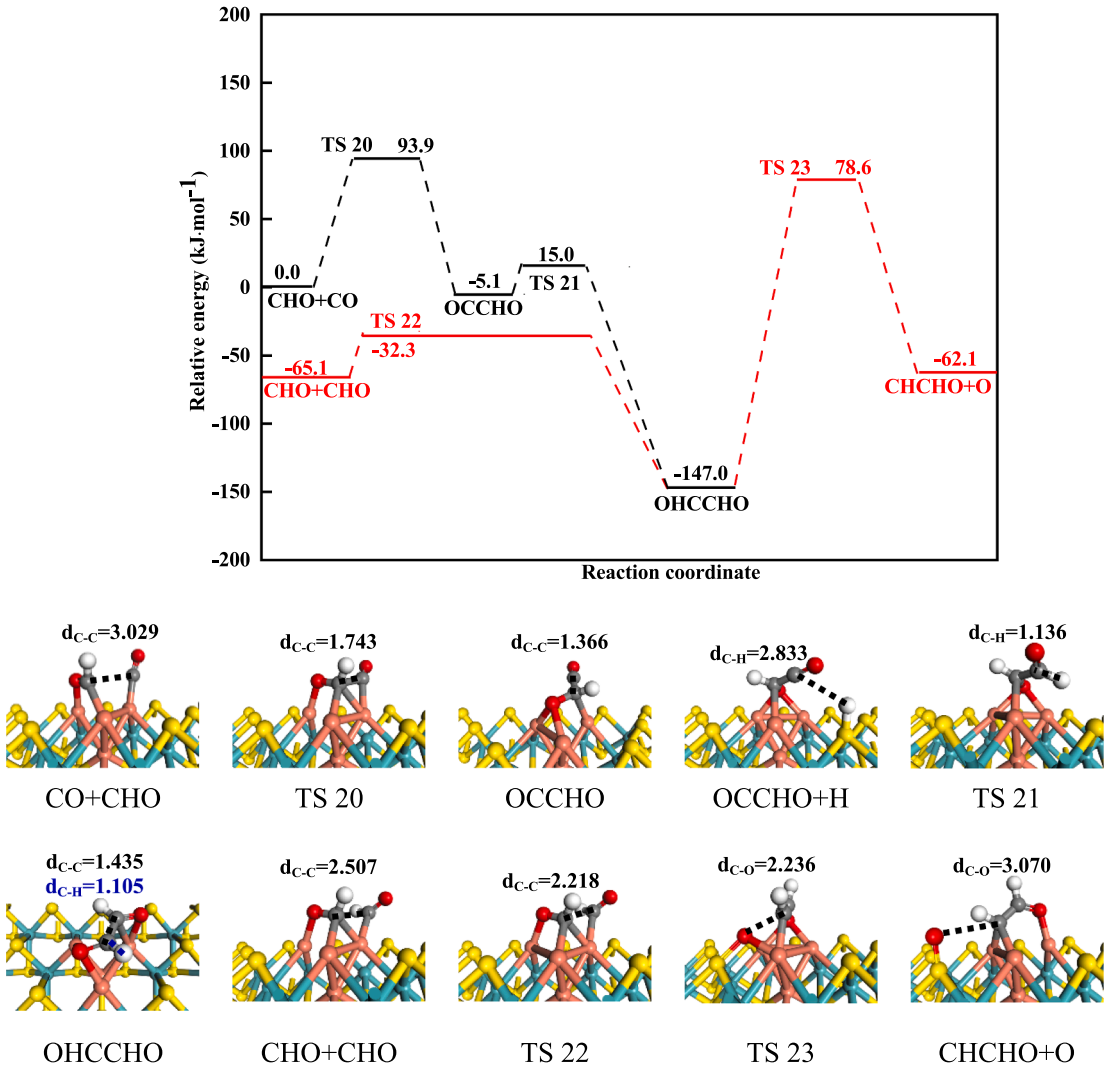

Fig. 8. The potential energy profile for CHCHO formation with the structures of the initial states (IS), transition states (TS), and final states (FS).

with the results of Noskov et al. [85], they found that the adsorption energy of N atom has a strong relationship related to the activation energy of direct dissociation of N_2, the greater the adsorption energy of N atoms was, the lower the activation energy of direct dissociation of N_2 was, and the higher the reaction rate of N_2 dissociation was.

3.6. Microstructure analysis

3.6.1. Influence of loaded Cu_4 clusters on adsorption of key intermediates

The adsorption energies of the key intermediates on the surfaces of $Cu_4/MoS_2(001)$ and $MoS_2(10–10)$ [28] surface during the ethanol synthesis reaction were analyzed, as shown in Table 3.

The adsorption energy of CHO, COH, CH_3CO and other substances on the $Cu_4/MoS_2(001)$ surface is higher than that on the $MoS_2(10–10)$ [28]. Therefore, Cu loading on the surface of MoS_2 catalyst could increase the adsorption energy of key species. The reaction energy barrier of CHO formed by initial CO activation on $Cu_4/MoS_2(001)$ is lower than that of $MoS_2(10–10)$ [28]. On these surfaces, the reaction energy barriers of CO activation are 111.0 and 139.9 kJ·mol^{-1}, which can be seen that the load of Cu promotes the activation of CO.

3.6.2. Charge analysis of $Cu_4/MoS_2(001)$ surface

Furthermore, the catalytic performance of Cu_4 modified MoS_2 catalyst was illustrated from the microscopic perspective, and the Bader charge and differential charge on $Cu_4/MoS_2(001)$ surface were calculated (Fig. 11).

In order to understand the electronic properties of $Cu_4/MoS_2(001)$ catalyst, we analyzed the difference of charge density on the surface of $Cu_4/MoS_2(001)$, the corresponding parameter is set to 0.005 e/Å^3 as shown in Fig. 11. The results showed that electron transfer occurred between Cu and MoS_2, and the charge gathered at the interface. Bader charge analysis shows that the total charge transfer from Cu_4 to MoS_2 is 0.43 *e*. Therefore, the analysis of electronic and structural properties shows that there is moderate charge transfer between Cu and MoS_2, and a charge region is formed at the interface of $Cu_4/MoS_2(001)$ catalyst, which improves the catalytic performance of syngas to ethanol.

3.6.3. The role of metal clusters and interfacial effects in ethanol synthesis

In the process of syngas conversion on $Cu_4/MoS_2(001)$ catalyst, CO is firstly adsorbed at the T position, and then CO is hydrogenated to form CHO, which is adsorbed at the Hol site of the Cu_4 cluster. It can be seen that the metal cluster is the active site of CO hydrogenation to form CHO. Subsequently, CH_2O is formed by CHO hydrogenation, which adsorbs at the Hol site of the Cu_4 cluster. The C-O bond in CH_2O is broken at the interface between Cu_4 metal cluster and MoS_2 to form CH_2 species after CH_2O reacted with the active H atom. In the subsequent reaction, CHO is adsorbed at the B site of the Cu_4 cluster, and CH_2 is adsorbed at the Hol_1 site between Cu and MoS_2. Finally, CHO is inserted into CH_2 to form CH_2CHO species. The results show that the interface between Cu_4 and MoS_2 promotes the H-assisted dissociation of CH_2O to

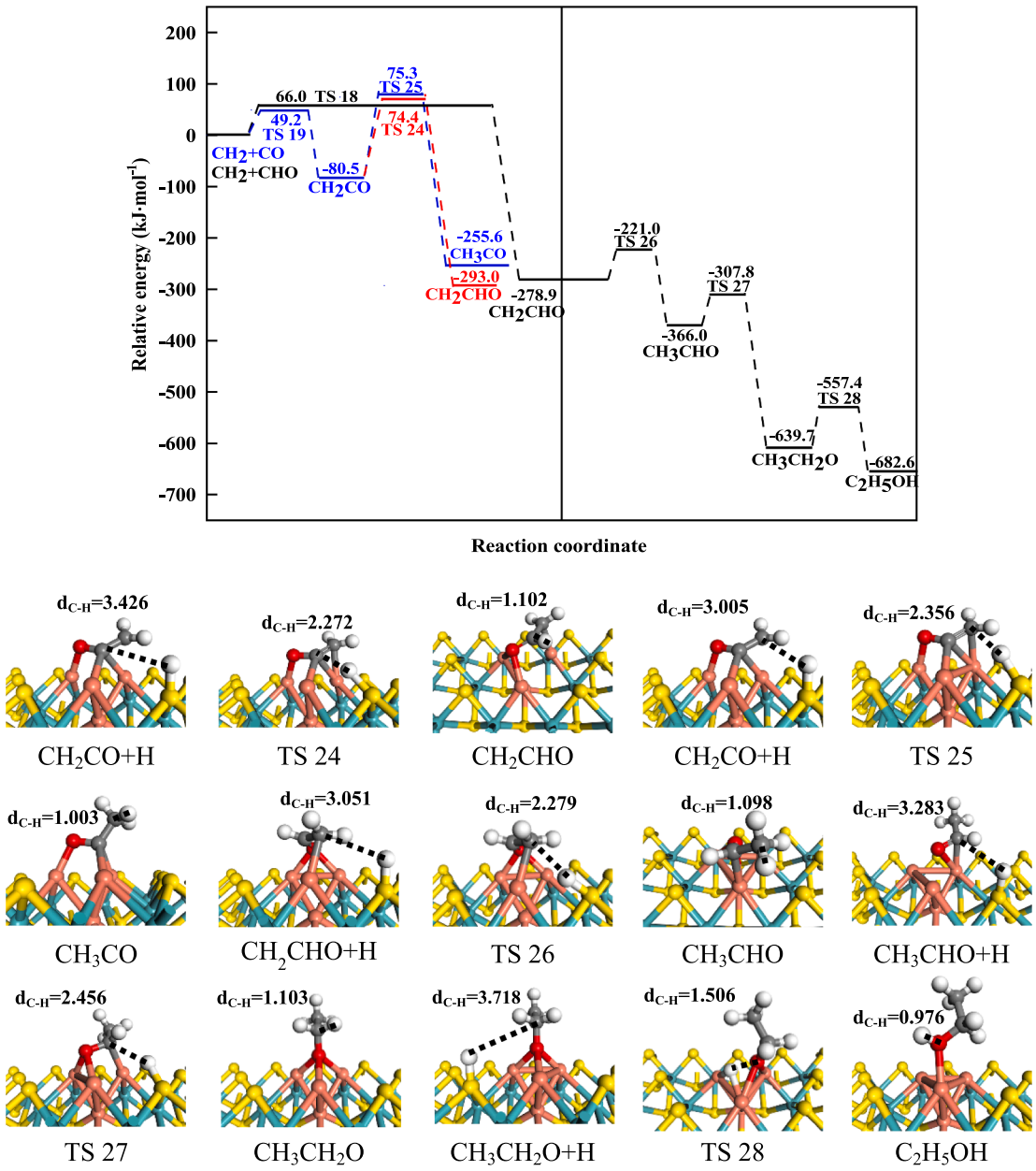

Fig. 9. The potential energy profile for ethanol formation from CH_2 species with the structures of the initial states (IS), transition states (TS), and final states (FS).

form CH_2, and provides the active site for CH_2CHO formation.

3.7. General discussion

In general, according to our calculation on the surface of $Cu_4/MoS_2(001)$, we can conclude that the formation of CH_2 is more favorable than the CH_3OH formation. Therefore, it can be obtained that CH_2 species participates in the insertion of CHO to form CH_2CHO, and then hydrogenation to ethanol continuously. At the same time, CH_3 generated by CH_2 hydrogenation is restrained on $Cu_4/MoS_2(001)$ surface due to the high activation barrier. The results show that Cu_4 clusters modified $MoS_2(001)$ surface can improve the selectivity of ethanol synthesis from syngas, facilitate the generation of CH_2 and insert into CHO, also reduce CH_3OH and CH_3 generation. Then, this work analyzes the reaction between the $MoS_2(001)$[31] and $Cu_4/MoS_2(001)$ surfaces, the results show that the Cu_4 clusters modified MoS_2 not only provides a new adsorption sites for the adsorption species, and apparently stable transition state of the product, the interface between Cu and MoS_2 reduces the activation barrier of CH_2 formation step, the Cu_4 clusters can promote the formation of CH_2 and CHO insertion, and restrain the CH_3 formation. Thus, the selectivity of synthesis ethanol from syngas are improved.

4. Conclusion

In this study, the reaction mechanism of synthesis of ethanol from syngas is calculated over the $Cu_4/MoS_2(001)$ surface by density functional theory. Our detailed results show that CO is initially activated to CHO, and the reaction barrier is 111.0 kJ·mol^{-1}. The formed CHO is preferentially dissociated by hydrogen to form CH_2, which is the major CH_x species. The rate-determining step of forming CH_2 species is $CH_2O + H \rightarrow CH_2 + OH$, with the reaction energy barrier of 77.4 kJ·mol^{-1}. In the related reaction of CH_2, the reactions of CH_2CHO and CH_2CO formation by the CHO and CO insert into CH_2 are more favorable than CH_3 formation by the CH_2 hydrogenation. Therefore, the formation of CH_2CHO and CH_2CO is promoted by Cu_4 metal cluster on Cu_4/MoS_2

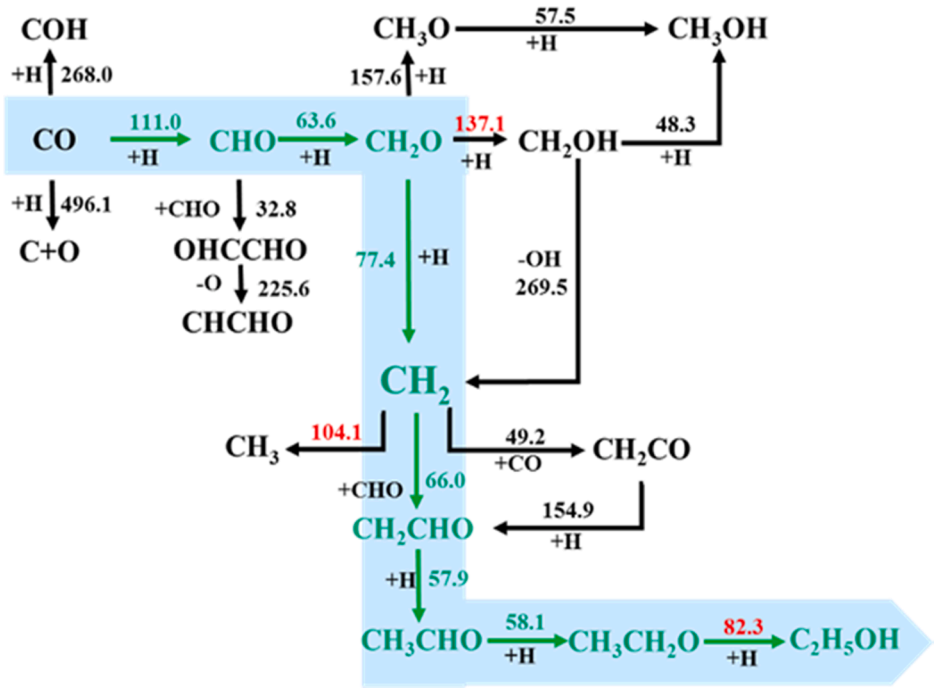

Fig. 10. The possible reaction pathways and related barriers (kJ·mol^{-1}) for syngas conversion on the $Cu_4/MoS_2(001)$ surface.

Table 1
Rate constants (s^{-1}) of key primitive reactions at different temperatures (K).

Reaction	673	723	773	823	873	923
CO + H → CHO	3.64 × 10^{-1}	1.43 × 10^{0}	4.73 × 10^{0}	1.35 × 10^{1}	3.42 × 10^{1}	7.82 × 10^{1}
CHO + H → CH_2O	1.78 × 10^{3}	3.80 × 10^{3}	7.35 × 10^{3}	1.31 × 10^{4}	2.20 × 10^{4}	3.48 × 10^{4}
CH_2O + H → CH_2 + OH	1.69 × 10^{3}	3.89 × 10^{3}	4.86 × 10^{3}	1.52 × 10^{4}	2.68 × 10^{4}	4.43 × 10^{4}
CH_2 + CHO → CH_2CHO	7.52 × 10^{2}	1.59 × 10^{3}	3.05 × 10^{3}	5.39 × 10^{3}	8.95 × 10^{3}	1.40 × 10^{4}
CH_2CHO + H → CH_3CHO	5.21 × 10^{3}	9.95 × 10^{3}	1.75 × 10^{4}	2.86 × 10^{4}	4.44 × 10^{4}	6.56 × 10^{4}
CH_3CHO + H → CH_3CH_2O	3.05 × 10^{3}	5.87 × 10^{3}	1.04 × 10^{4}	1.71 × 10^{4}	2.67 × 10^{4}	3.96 × 10^{4}
CH_3CH_2O + H → C_2H_5OH	4.10 × 10^{2}	8.81 × 10^{2}	1.71 × 10^{3}	3.08 × 10^{3}	5.17 × 10^{3}	8.21 × 10^{3}
CH_2O + H → CH_2OH	2.23 × 10^{0}	9.85 × 10^{0}	3.59 × 10^{1}	1.12 × 10^{2}	3.06 × 10^{2}	7.49 × 10^{2}
CH_2OH + H → CH_3OH	3.59 × 10^{4}	6.01 × 10^{4}	9.41 × 10^{4}	1.40 × 10^{5}	1.98 × 10^{5}	2.70 × 10^{5}
CH_2 + H → CH_3	3.34 × 10^{0}	1.10 × 10^{1}	3.09 × 10^{1}	7.66 × 10^{1}	1.71 × 10^{1}	3.51 × 10^{2}

Table 2
The adsorption energy of key species on $Cu_4/MoS_2(001)$ surfaces.

Species	Adsorption energy (E_{ads}/kJ·mol^{-1})
CH_2OH	−205.6
CH_2	−346.5
CH_3	−218.9
CH_2CHO	−262.8

catalyst. The optimal reaction path to form ethanol is: CHO + H → CH_2O; CH_2O + H → CH_2 + OH; CH_2 + CHO → CH_2CHO; CH_2CHO + H → CH_3CHO; CH_3CHO + H → CH_3CH_2O; CH_3CH_2O + H → C_2H_5OH. The rate-determining step is CH_3CH_2O + H → C_2H_5OH among all elementary reactions, with the reaction barrier of 82.3 kJ·mol^{-1}. For the methanol formation, the step with the highest energy barrier is CH_2O + H → CH_2OH, which needs to overcome the energy barrier of 137.1 kJ·mol^{-1}.

Table 3
The adsorption energy (E_{ads}/kJ·mol^{-1}) of partially reactive species on MoS_2(10–10) [28] and $Cu_4/MoS_2(001)$ surfaces.

Species	MoS_2(10–10)	$Cu_4/MoS_2(001)$
CHO	−193.9	−306.8
COH	−261.5	−271.0
CHOH	−250.9	−324.2
CH_2O	−48.2	−71.4
CH_2OH	−192.0	−205.6
CH_3CO	−191.0	−200.3
CH_3CHO	−38.6	−61.8

The catalytic effect of Cu-modified MoS_2 catalyst on the formation of ethanol is mainly manifested in the fact that Cu provided undissociated CHO, and the reaction of CH_2 inserted into CHO to form CH_2CHO also occurred at the boundary of the Cu_4 and MoS_2. Namely, the synergistic effect of Cu and MoS_2 promotes the insertion of CHO into CH_2. The electron structure analysis shows that there is a strong electron transfer between Cu_4 and MoS_2, which increases the interaction between Cu_4 and $MoS_2(001)$ and improves the adsorption energy of the reaction species on the catalyst surface. At the same time, there is a charge accumulation region between the Cu_4 cluster and MoS_2, and the selectivity of C_2 oxygenates can be improved at this interface.

CRediT authorship contribution statement

Jiawang Chen: Data curation, Writing - original draft, Validation, Formal analysis, Investigation. **Zhanhui Wang:** Investigation, Formal analysis. **Juan Zhao:** Formal analysis. **Lixia Ling:** Writing - review & editing, Investigation, Project administration, Funding acquisition. **Riguang Zhang:** Methodology. **Baojun Wang:** Software, Conceptualization, Resources, Funding acquisition.

Declaration of Competing Interest

The authors declare that they have no known competing financial interests or personal relationships that could have appeared to influence the work reported in this paper.

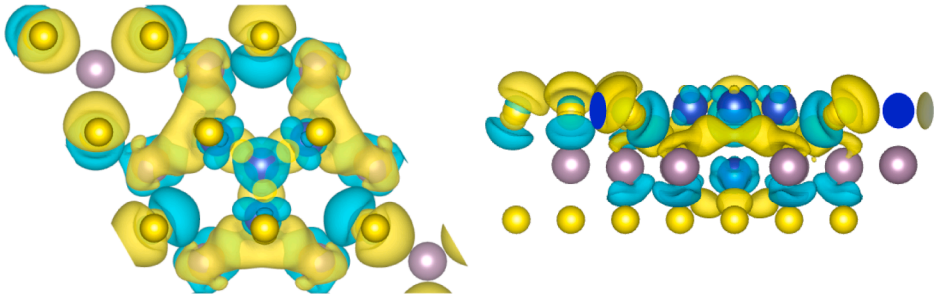

Fig. 11. Differential charge density of $Cu_4/MoS_2(001)$ surface. Blue and yellow shaded regions represent the charge gain and charge loss, respectively. (For interpretation of the references to colour in this figure legend, the reader is referred to the web version of this article.)

Acknowledgements

This work is financially supported by the Key projects of National Natural Science Foundation of China (No. 21736007), the National Natural Science Foundation of China (Grant Nos. 21576178 and 21476155), Research Project Supported by Shanxi Scholarship Council of China (No. 2016-030).

References

[1] M. Ao, G.H. Pham, J. Sunarso, M.O. Tade, S. Liu, Active Centers of Catalysts for Higher Alcohol Synthesis from Syngas: A Review, ACS Catal. 8 (8) (2018) 7025–7050.
[2] E. Bertheussen, A. Verdaguer-Casadevall, D. Ravasio, J.H. Montoya, D.B. Trimarco, C. Roy, S. Meier, J. Wendland, J.K. Nørskov, I.E.L. Stephens, I.b. Chorkendorff, Acetaldehyde as an Intermediate in the Electroreduction of Carbon Monoxide to Ethanol on Oxide-Derived Copper, Angew. Chem. 128 (4) (2016) 1472–1476.
[3] J. Gong, H. Yue, Y. Zhao, S. Zhao, L.i. Zhao, J. Lv, S. Wang, X. Ma, Synthesis of Ethanol via Syngas on Cu/SiO 2 Catalysts with Balanced Cu 0 –Cu + Sites, JACS 134 (34) (2012) 13922–13925.
[4] R. Zhang, G. Wang, B. Wang, Insights into the mechanism of ethanol formation from syngas on Cu and an expanded prediction of improved Cu-based catalyst, J. Catal. 305 (2013) 238–255.
[5] J. Wang, Q. Sun, S. Chan, H. Su, The acceleration of methanol synthesis and C_2 oxygenates formation on copper grain boundary from syngas, Appl. Catal. A 509 (2016) 97–104.
[6] T. Cheng, H. Xiao, W.A. Goddard, Nature of the Active Sites for CO Reduction on Copper Nanoparticles; Suggestions for Optimizing Performance, JACS 139 (34) (2017) 11642–11645.
[7] YongMan Choi, P. Liu, Mechanism of Ethanol Synthesis from Syngas on Rh(111), JACS 131 (36) (2009) 13054–13061.
[8] N. Yang, A.J. Medford, X. Liu, F. Studt, T. Bligaard, S.F. Bent, J.K. Nørskov, Intrinsic Selectivity and Structure Sensitivity of Rhodium Catalysts for C $_{2+}$ Oxygenate Production, JACS 138 (11) (2016) 3705–3714.
[9] N.Y. Yang, J.S. Yoo, J. Schumann, P. Bothra, J.A. Singh, E. Balle, F. Abild-Pedersen, J.K. Nørskov, S.F. Bent, Interface sites formed by atomic layer deposition promote syngas conversion to higher oxygenates, ACS Catal. 7 (2017) 5746–5757.
[10] R.G. Zhang, M. Peng, B.J. Wang, Catalytic selectivity of Rh/TiO_2 catalyst in syngas conversion to ethanol: probing into the mechanism and functions of TiO_2 support and promoter, Catal. Sci. Technol. 7 (2017) 1073–1085.
[11] H. Shou, D. Ferrari, D.G. Barton, C.W. Jones, R.J. Davis, Influence of Passivation on the Reactivity of Unpromoted and Rb-Promoted Mo 2 C Nanoparticles for CO Hydrogenation, ACS Catal. 2 (7) (2012) 1408–1416.
[12] V.P. Santos, B.V.D. Linden, A. Chojecki, G. Budroni, S. Corthals, H. Shibata, G. R. Meima, K. Kapteijn, M. Makkee, J. Gascon, Mechanistic Insight into the synthesis of higher alcohols from syngas: the role of K promotion on MoS_2 catalysts, ACS Catal. 3 (2013) 1634–1637.
[13] M. Konarova, F.Q. Tang, J.L. Chen, G. Wang, V. Rudolph, J. Beltramini, Nano- and microscale engineering of the molybdenum disulfide-based catalysts for syngas to ethanol conversion, Chem Cat Chem. 6 (2014) 2394–2402.
[14] V.S. Dorokhov, E.A. Permyakov, P.A. Nikulshin, V.V. Maximov, V.M. Kogan, Experimental and computational study of syngas and ethanol conversion mechanisms over K-modified transition metal sulfide catalysts, J. Catal. 344 (2016) 841–853.
[15] S.F. Zaman, N. Pasupulety, A.A. Al-Zahrani, M.A. Daous, S.S. Al-Shahrani, H. Driss, L.A. Petrov, K.J. Smith, Carbon monoxide hydrogenation on potassium promoted Mo 2 N catalysts, Appl. Catal. A 532 (2017) 133–145.
[16] Z. Zhao, W. Lu, R. Yang, H. Zhu, W. Dong, F. Sun, Z. Jiang, Y. Lyu, T. Liu, H. Du, Y. Ding, Insight into the Formation of Co@Co 2 C Catalysts for Direct Synthesis of Higher Alcohols and Olefins from Syngas, ACS Catal. 8 (1) (2018) 228–241.
[17] Y.-P. Pei, J.-X. Liu, Y.-H. Zhao, Y.-J. Ding, T. Liu, W.-D. Dong, H.-J. Zhu, H.-Y. Su, L. I. Yan, J.-L. Li, W.-X. Li, High Alcohols Synthesis via Fischer–Tropsch Reaction at Cobalt Metal/Carbide Interface, ACS Catal. 5 (6) (2015) 3620–3624.
[18] R.G. Zhang, G.X. Wen, H. Adidharma, A.G. Russell, B.J. Wang, M. Radosz, M. H. Fan, C_2 oxygenate synthesis via Fischer-Tropsch synthesis on Co_2C and Co/Co_2C interface catalysts: how to control the catalyst crystal facet for optimal selectivity, ACS Catal. 7 (2017) 8285–8295.
[19] R. Burch, M.J. Hayes, The Preparation and Characterisation of Fe-Promoted Al_2O_3-Supported Rh Catalysts for the Selective Production of Ethanol from Syngas, J. Catal. 165 (2) (1997) 249–261.
[20] D.C.D. da Silva, S. Letichevsky, L.E.P. Borges, L.G. Appel, The Ni/ZrO_2 catalyst and the methanation of CO and CO_2, Int. J. Hydrogen Energy 37 (11) (2012) 8923–8928.
[21] C. Li, J. Liu, W.a. Gao, Y. Zhao, M. Wei, Ce-Promoted Rh/TiO_2 Heterogeneous Catalysts Towards Ethanol Production from Syngas, Catal Lett 143 (11) (2013) 1247–1254.
[22] R. Quinn, T.A. Dahl, B.A. Toseland, An evaluation of synthesis gas contaminants as methanol synthesis catalyst poisons, Appl. Catal. A 272 (1-2) (2004) 61–68.
[23] Y. Ma, Q. Ge, W. Li, H. Xu, Study on the sulfur tolerance of catalysts for syngas to methanol, Catal. Commun. 10 (1) (2008) 6–10.
[24] J.M. Christensen, P.M. Mortensen, R. Trane, P.A. Jensen, A.D. Jensen, Effects of H_2S and process conditions in the synthesis of mixed alcohols from syngas over alkali promoted cobalt-molybdenum sulfide, Appl. Catal. A 366 (1) (2009) 29–43.
[25] M. Feng, Review of Molybdenum Catalysts for Direct Synthesis of Mixed Alcohols from Synthesis Gas, RPCAT 1 (1) (2012) 13–26.
[26] X.u. Xiaoding, E.B.M. Doesburg, J.J.F. Scholten, Synthesis of higher alcohols from syngas - recently patented catalysts and tentative ideas on the mechanism, Catal. Today 2 (1) (1987) 125–170.
[27] S.W. Chiang, C.C. Chang, J.L. Shie, C.Y. Chang, D.R. Ji, J.Y. Tseng, C.F. Chang, Y.H. Chen, Synthesis of alcohols and alkanes from CO and H2 over MoS2/γ-Al2O3 catalyst in a packed bed with continuous flow, Energies 5 (2012) 4147-4164.
[28] X.R. Shi, H.J. Jiao, K. Hermann, J.G. Wang, CO hydrogenation reaction on sulfided molybdenum catalysts, J. Mol. Catal. A-Chem. 312 (2009) 7-17.
[29] Z. Li, K. Zhang, W. Wang, B. Wang, X. Ma, DFT study into the reaction mechanism of CO methanation over pure MoS 2, Int J Quantum Chem 118 (16) (2018) e25643, https://doi.org/10.1002/qua.v118.1610.1002/qua.25643.
[30] M. Huang, K. Cho, Density Functional Theory Study of CO Hydrogenation on a MoS 2 Surface, J. Phys. Chem. C 113 (13) (2009) 5238–5243.
[31] K. Zhang, Q. Wang, B. Wang, Y. Xu, X. Ma, Z. Li, A DFT study on CO methanation over the activated basal plane from a strained two-dimensional nano-MoS_2, Appl. Surf. Sci. 479 (2019) 360–367.
[32] Y.-Y. Chen, X. Zhao, X.-D. Wen, X.-R. Shi, M. Dong, J. Wang, H. Jiao, Mechanistic aspect of ethanol synthesis from methanol under CO hydrogenation condition on MoS_x cluster model catalysts, J. Mol. Catal. A: Chem. 329 (1-2) (2010) 77–85.
[33] V.R. Surisetty, I. Eswaramoorthi, A.K. Dalai, Comparative study of higher alcohols synthesis over alumina and activated carbon-supported alkali-modified MoS_2 catalysts promoted with group VIII metals, Fuel 96 (2012) 77–84.
[34] J. Mao, Y. Wang, Z.L. Zheng, D.H. Deng, The rise of two-dimensional MoS_2 for catalysis, Front. Phys. 13 (4) (2018) 138118–138137.
[35] J. Iranmahboob, H. Toghiani, D.O. Hill, Dispersion of alkali on the surface of Co-MoS_2/clay catalyst: a comparison of K and Cs as a promoter for synthesis of alcohol, Appl. Catal., A 247 (2003) 207–218.
[36] J. Iranmahboo, D.O. Hill, Alcohol synthesis from syngas over $K_2CO_3/CoS/MoS_2$ on activated carbon, Catal. Lett. 78 (2002) 49–55.
[37] K.J. Smith, R.G. Herman, K. Klier, Kinetic modelling of higher alcohol synthesis over alkali-promoted Cu/ZnO and MoS_2 catalysts, Chem. Eng. Sci. 45 (1990) 2639–2646.
[38] S. Park, J. Park, H. Abroshan, L. Zhang, J.K. Kim, J. Zhang, J. Guo, S. Siahrostami, X. Zheng, Enhancing Catalytic Activity of MoS 2 Basal Plane S-Vacancy by Co Cluster Addition, ACS Energy Lett. 3 (11) (2018) 2685–2693.
[39] M.B. Gawande, A. Goswami, F.X. Felpin, T. Asefa, X.X. Huang, R. Silva, X.X. Zou, R. Zboril, R.S. Varma, Cu and Cu-based nanoparticles: synthesis and applications in catalysis, Chem. Rev. 116 (2016) 3722–3811.

[40] J. Yoshihara, C.T. Campbell, Methanol synthesis and reverse Water-Gas Shift kinetics over Cu(110) model catalysts: structural sensitivity, J. Catal. 161 (1996) 776–782.
[41] X. Sun, R. Zhang, B. Wang, Insights into the preference of CHx(x=1–3) formation from CO hydrogenation on Cu(111) surface, Appl. Surf. Sci. 265 (2013) 720–730.
[42] R. Zhang, X. Sun, B. Wang, Insight into the Preference Mechanism of CH x (x = 1–3) and C–C Chain Formation Involved in C 2 Oxygenate Formation from Syngas on the Cu(110) Surface, J. Phys. Chem. C 117 (13) (2013) 6594–6606.
[43] H. Zheng, R. Zhang, Z. Li, B. Wang, Insight into the mechanism and possibility of ethanol formation from syngas on Cu(100) surface, J. Mol. Catal. A: Chem. 404-405 (2015) 115–130.
[44] R.G. Zhang, F. Liu, B.J. Wang, Co-decorated Cu alloy catalyst for C_2 oxygenate and ethanol formation from syngas on Cu-based catalyst: insight into the role of Co and Cu as well as the improved selectivity, Catal. Sci. Technol. 6 (2016) 8036–8054.
[45] V. Mahdavi, M.H. Peyrovi, M. Islami, J.Y. Mehr, Synthesis of higher alcohols from syngas over Cu-Co_2O_3/ZnO, Al_2O_3 catalyst, Appl. Catal. A 281 (1-2) (2005) 259–265.
[46] B. Ren, X. Dong, Y. Yu, G. Wen, M. Zhang, A density functional theory study on the carbon chain growth of ethanol formation on Cu-Co (111) and (211) surfaces, Appl. Surf. Sci. 412 (2017) 374–384.
[47] Y.-H. Zhao, M.-M. Yang, D. Sun, H.-Y. Su, K. Sun, X. Ma, X. Bao, W.-X. Li, Rh-Decorated Cu Alloy Catalyst for Improved C 2 Oxygenate Formation from Syngas, J. Phys. Chem. C 115 (37) (2011) 18247–18256.
[48] R.G. Zhang, G.R. Wang, B.J. Wang, L.X. Ling, Insight into the effect of promoter Mn on ethanol formation from syngas on a Mn-promoted MnCu(211) surface: a comparison with a Cu(211) surface, J. Phys. Chem. C 118 (2014) 5243–5254.
[49] T. Schalow, B. Brandt, D.E. Starr, M. Laurin, S.K. Shaikhutdinov, S. Schauermann, J. Libuda, H.J. Freund, Size-dependent oxidation mechanism of supported Pd nanoparticle, Angew. Chem. Int. Ed. 45 (2006) 3693–3697.
[50] J.A. Rodriguez, P. Liu, Y. Takahashi, F. Viñes, L. Feria, E. Florez, K. Nakamura, F. Illas, Novel Au–TiC catalysts for CO oxidation and desulfurization processes, Catal. Today 166 (1) (2011) 2–9.
[51] C. Liu, B. Yang, E. Tyo, S. Seifert, J. DeBartolo, B. von Issendorff, P. Zapol, S. Vajda, L.A. Curtiss, Carbon Dioxide Conversion to Methanol over Size-Selected Cu 4 Clusters at Low Pressures, JACS 137 (27) (2015) 8676–8679.
[52] I. Kasatkin, B. Kniep, T. Ressler, Cu/ZnO and Cu/ZrO 2 interactions studied by contact angle measurement with TEM, PCCP 9 (7) (2007) 878–883.
[53] A.B. Vidal, L. Feria, J. Evans, Y. Takahashi, P. Liu, K. Nakamura, F. Illas, J. A. Rodriguez, CO_2 activation and methanol dynthesis on novel Au/TiC and Cu/TiC catalysts, J. Phys. Chem. Lett. 3 (2012) 2275–2280.
[54] K.M. Neyman, C. Inntam, L.V. Moskaleva, N. Rçsch, Density functional embedded cluster study of Cu_4, Ag_4 and Au_4 species interacting with oxygen vacancies on the MgO(001) surface, Chem. Eur. J. 13 (2007) 277–286.
[55] C. Inntam, L.V. Moskaleva, I.V. Yudanov, K.M. Neyman, N. Rösch, Adsorption of Cu_4, Ag_4 and Au_4 particles on the regular MgO(001) surface: a density functional study using embedded cluster models, Chem. Phys.Lett. 417 (2006) 515–520.
[56] G. Geudtner, K. Jug, A.M. Köster, Cu adsorption on the MgO(100) surface, Surface Science 467 (1-3) (2000) 98–106.
[57] A.V. Matveev, K.M. Neyman, G. Pacchioni, N. Rösch, Density functional study of M_4 clusters (M=Cu, Ag, Ni, Pd) deposited on the regular MgO(001) surface, Chem. Phys. Lett. 299 (6) (1999) 603–612.
[58] A. Del Vitto, C. Sousa, F. Illas, G. Pacchioni, Optical properties of Cu nanoclusters supported on MgO(100), J. Chem. Phys. 121 (15) (2004) 7457–7466.
[59] R. Zhang, T. Duan, B. Wang, L. Ling, Unraveling the role of support surface hydroxyls and its effect on the selectivity of C_2 species over Rh/γ-Al_2O_3 catalyst in syngas conversion: A theoretical study, Appl. Surf. Sci. 379 (2016) 384–394.
[60] Y. Lu, R. Zhang, B. Cao, B. Ge, F.F. Tao, J. Shan, L. Nguyen, Z. Bao, T. Wu, J. W. Pote, B. Wang, F. Yu, Elucidating the Copper–Hägg Iron Carbide Synergistic Interactions for Selective CO Hydrogenation to Higher Alcohols, ACS Catal. 7 (8) (2017) 5500–5512.
[61] T.-Y. Chen, J. Su, Z. Zhang, C. Cao, X.u. Wang, R. Si, X. Liu, B. Shi, J. Xu, Y.-F. Han, Structure Evolution of Co–CoO x Interface for Higher Alcohol Synthesis from Syngas over Co/CeO 2 Catalysts, ACS Catal. 8 (9) (2018) 8606–8617.
[62] N. Koizumi, G.Z. Bian, K. Murai, T. Ozaki, M. Yamada, In situ DRIFT studies of sulfided K-Mo/γ-A1$_2$O$_3$ catalysts, J. Mol. Catal. A-Chem. 207 (2004) 173–182.
[63] A.K. Gunturu, E.L. Kugler, J.B. Cropley, D.B. Dadyburjor, A Kinetic Model for the Synthesis of High-Molecular-Weight Alcohols over a Sulfided Co−K−Mo/C Catalyst, Ind. Eng. Chem. Res. 37 (6) (1998) 2107–2115.
[64] F. Calle-Vallejo, M.T.M. Koper, Theoretical Considerations on the Electroreduction of CO to C 2 Species on Cu(100) Electrodes, Angew. Chem. Int. Ed. 52 (28) (2013) 7282–7285.
[65] E. Pérez-Gallent, M.C. Figueiredo, F. Calle-Vallejo, M.T.M. Koper, Spectroscopic Observation of a Hydrogenated CO Dimer Intermediate During CO Reduction on Cu(100) Electrodes, Angew. Chem. Int. Ed. 56 (13) (2017) 3621–3624.
[66] G. Kresse, J. Hafner, Ab initio molecular dynamics for liquid metals, Phys. Rev. B 48 (1993) 13115–13118.
[67] G. Kresse, J. Furthmüller, Efficient iterative schemes for ab initio total-energy calculations using a plane-wave basis set, Phys. Rev. B 54 (16) (1996) 11169–11186.
[68] G. Kresse, J. Furthmuller, Efficiency of ab-initio total energy calculations for metals and semiconductors using a plane-wave basis set, Mater. Sci. 6 (1996) 15–50.
[69] J.P. Perdew, J.A. Chevary, S.H. Vosko, K.A. Jackson, M.R. Pederson, D.J. Singh, C. Fiolhais, Atoms, molecules, solids, and surfaces: applications of the generalized gradient approximation for exchange and correlation, Phys. Rev. B. 46 (1992) 6671–6687.
[70] M. Methfessel, A.T. Paxton, High-precision sampling for Brillouin-zone integration in metals, Phys. Rev. B 40 (6) (1989) 3616–3621.
[71] D. Sheppard, P. Xiao, W. Chemelewski, D.D. Johnson, G. Henkelman, A generalized solid-state nudged elastic band method, J. Chem. Phys. 136 (7) (2012) 074103, https://doi.org/10.1063/1.3684549.
[72] D. Sheppard, R. Terrell, G. Henkelman, Optimization methods for finding minimum energy paths, J. Chem. Phys. 128 (13) (2008) 134106, https://doi.org/10.1063/1.2841941.
[73] G. Henkelman, H. Jónsson, A dimer method for finding saddle points on high dimensional potential surfaces using only first derivatives, J. Chem. Phys. 111 (15) (1999) 7010–7022.
[74] R.A. Olsen, G.J. Kroes, G. Henkelman, A. Arnaldsson, H. Jónsson, Comparison of methods for finding saddle points without knowledge of the final states, J. Chem. Phys. 121 (20) (2004) 9776–9792.
[75] S. Reshmi, M.V. Akshaya, B. Satpati, P.K. Basu, K. Bhattacharjee, Structural stability of coplanar 1T–2H superlattice MoS_2 under high energy electron beam, Nanotechnology. 29 (2018) 205604–205618.
[76] C. Zhang, P. Li, X. Liu, T. Liu, Z. Jiang, C. Li, Morphology-performance relation of (Co)MoS_2 catalysts in the hydrodesulfurization of FCC gasoline, Appl. Catal. A 556 (2018) 20–28.
[77] S. Wang, D.i. Zhang, B. Li, C. Zhang, Z. Du, H. Yin, X. Bi, S. Yang, Ultrastable In-Plane 1T-2H MoS 2 Heterostructures for Enhanced Hydrogen Evolution Reaction, Adv. Energy Mater. 8 (25) (2018) 1801345, https://doi.org/10.1002/aenm.v8.2510.1002/aenm.201801345.
[78] C.Y. Liu, Y.Z. Tan, S.S. Lin, H. Li, X.J. Wu, L. Li, Y. Pei, X.C. Zeng, CO self-promoting oxidation on nanosized gold clusters: triangular Au_3 active site and CO induced O-O scission, JACS 135 (2013) 2583–2595.
[79] Z.W. Chen, J.M. Yan, W.T. Zheng, Q. Jiang, Cu_4 Cluster Doped Monolayer MoS_2 for CO Oxidation, Sci Rep 5 (1) (2015), https://doi.org/10.1038/srep11230.
[80] A. Andersen, S.M. Kathmann, M.A. Lilga, K.O. Albrecht, R.T. Hallen, D.H. Mei, Effects of potassium doping on CO hydrogenation over MoS_2 catalysts: a first-principles investigation, Catal. Commun. 52 (2017) 92–97.
[81] K. Zhang, W.H. Wang, B.W. Wang, X.B. Ma, Z.H. Li, Promoted effect of cobalt on surface (010) of MoS_2 for CO methanation from a DFT study, Appl. Surf. Sci. 463 (2019) 635–646.
[82] L. Yang, P. Liu, Synthesis from syngas on transition metal-doped Rh(111) surfaces: a density functional kinetic monte carlo study, Top Catal. 57 (2014) 125–134.
[83] H. Bai, M. Ma, B. Bai, H. Cao, L. Zhang, Z. Gao, V.A. Vinokurov, W. Huang, Carbon chain growth by formyl coupling over the Cu/γ-AlOOH(001) surface in syngas conversion, PCCP 21 (1) (2019) 148–159.
[84] J.C. Wang, Z.X. Liu, R.G. Zhang, B.J. Wang, Ethanol synthesis from syngas on the stepped Rh(211) surface: effect of surface structure and composition, J. Phys. Chem. C 118 (2014) 22691–22701.
[85] K. Honkala, A. Hellman, I.N. Remediakis, A. Logadottir, A. Carlsson, S. Dahl, C. H. Christensen, J.K. Nørskov, Ammonia synthesis from First-Principles calculations, Sci. 307 (2005) 555–558.